Applied Radiation and Isotopes 69 (2011) 1668–1671

Contents lists available at ScienceDirect

Applied Radiation and Isotopes

journal homepage: www.elsevier.com/locate/apradiso

AB-BNCT beam shaping assembly based on $^{7}Li(p,n)^{7}Be$ reaction optimization

D.M. Minsky [a,b,c,*], A.J. Kreiner [a,b,c], A.A. Valda [a,b]

[a] Gerencia de Investigación y Aplicaciones, CNEA, Av. Gral Paz 1499 (B1650KNA), San Martín, Buenos Aires, Argentina
[b] Escuela de Ciencia y Tecnología, UNSAM, M. de Irigoyen 3100 (1650), San Martín, Argentina
[c] CONICET, Av. Rivadavia 1917 (C1033AAJ), Buenos Aires, Argentina

ARTICLE INFO

Available online 8 March 2011

Keywords:
Accelerator based-BNCT
$^{7}Li(p,n)^{7}B$ reaction
Beam shaping assembly

ABSTRACT

A numerical optimization of a Beam Shaping Assembly (BSA) for Accelerator Based-Boron Neutron Capture Therapy (AB-BNCT) has been performed. The reaction $^{7}Li(p,n)^{7}Be$ has been considered using a proton beam on a lithium fluoride target. Proton energy and the dimensions of a simple BSA geometry have been varied to obtain a set of different configurations. The optimal configuration of this set is shown.

1. Introduction

In the framework of *Accelerator Based-Boron Neutron Capture Therapy* (AB-BNCT) the $^{7}Li(p,n)^{7}Be$ reaction is the optimal reaction for neutron production for the treatment of deep seated tumors. Since this reaction is endothermic, the resulting neutron energy spectrum can be chosen to be as soft as desired by working near the reaction threshold. On the other hand larger proton beam energies lead to larger yields. The optimal energy will be a balance between the better primary spectra obtained by low proton energies and the bigger neutron yields associated with larger energies.

2. Materials and methods

2.1. $^{7}Li(p,n)^{7}Be$ neutron yield spectra

The neutron source used for the simulations is based on the reaction of protons on a lithium fluoride target. Neutrons emitted in the target are the starting point in the BSA simulations. The neutron yield and neutron energy–angular spectra for different energies have been calculated following Lee and Zhou (1999) but using more recent cross section data and including the excited state channel $^{7}Li(p,n)^{7}Be^{*}$. For the reaction leading to the ground state of ^{7}Be, Sekharan et al. (1976) data was considered for proton energies between 1.925 and 2.1 MeV, Abramovich et al. (1984) cross sections were used for proton energies above this energy and the cross section model adopted by Lee was considered for energies below 1.925 MeV. Cross sections from Liskien and Paulsen (1975) were used for the channel $^{7}Li(p,n)^{7}Be^{*}$. Liskien and Paulsen Legendre coefficients for angular distributions were used for both channels. Stopping powers were calculated using the SRIM 2008 code (Ziegler et al., 2008).

Energy and solid angle differential neutron yields have been calculated every 1 keV from 0 and up to the maximum neutron energy and for all azimuth angles in 1° steps. Those data organized in matrices were post-processed by Perl scripts in order to produce MCNP 5 (Brown et al., 2002) data cards for the neutron source. The MCNP data cards were defined in order that the linear interpolation performed in the distribution by MCNP does not exceed 1% error in the energy distributions and 2% in the angular distributions referring to the matrices. Angular distributions were defined every 10 keV.

Neutron sources for proton energies from 2.0 up to 2.8 MeV in steps of 0.1 MeV have been calculated.

2.2. Beam shaping assembly optimization

A modified Snyder head phantom (Goorley, 2002) was considered as a representation of a patient. The ^{10}B concentrations were assumed to be 65 ppm for tumor and 18 ppm for healthy tissue, and the CBEs/RBEs were 1.3 and 3.8 for boron dose in healthy tissue and tumor, respectively, 3.2 for the $^{14}N(n,p)^{14}C$ reaction and 3.2 for elastic scattering in hydrogen to be consistent with Binns et al. (2007). ICRU 46 (1992) tissue compositions were used for the scalp, skull and brain.

The beam shaping assembly (Fig. 1) consists in a cuboid of moderating materials surrounded by a lead reflector and with an enriched ^{6}Li lithium carbonate filter. The moderator is formed by successive layers of aluminum, PTFE and lithium carbonate.

* Corresponding author at: Gerencia de Investigación y Aplicaciones, CNEA, Av. Gral Paz 1499 (B1650KNA), San Martín, Buenos Aires, Argentina.
Tel.: +54 11 6772 7913; fax: +54 11 6772 7121.
E-mail address: minsky@tandar.cnea.gov.ar (D.M. Minsky).

0969-8043/$ - see front matter © 2011 Elsevier Ltd. All rights reserved.
doi:10.1016/j.apradiso.2011.02.047

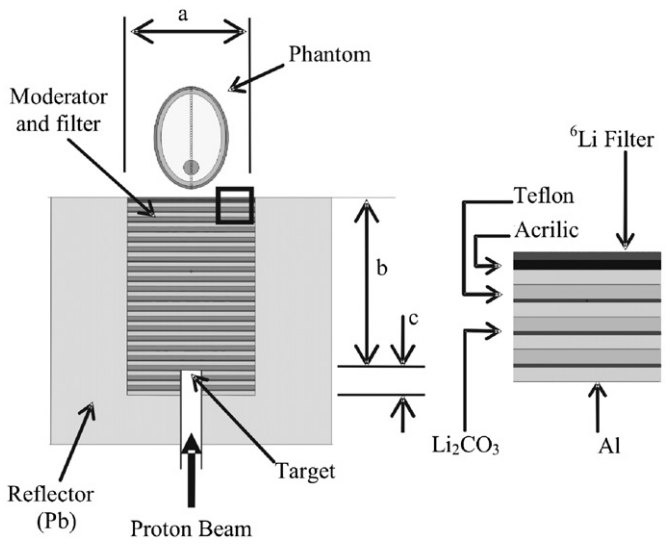

Fig. 1. Left: BSA and phantom considered in the simulations. Right: Detail of the moderator layers.

Different configurations have been generated by varying not only the energy of the protons, and hence the spectra of the neutrons, but also some geometry parameters:

- the beam port width (a) has been varied from 5 to 30 cm in 5 cm steps;
- the distance from the target up to the neutron port (b), was varied from 15 to 45 cm in 5 cm steps;
- the distance from the target up to the back of the moderator (c) was analyzed for 1, 5 and 10 cm.

Combining dimensions and proton energies a total of 1134 configurations were generated.

For each configuration the dose for healthy and tumor tissues vs. the depth inside the phantom have been simulated by MCNP 5 1.40 Monte Carlo transport code (Brown et al., 2002). A 30 mA proton beam current was considered for the normalizations since there is a project under development for building an accelerator capable of delivering this current in our group (Kreiner et al., 2010). The optimal configuration was chosen as the one that can treat tumors in the biggest range of depth and with treatment times shorter than 60 min.

3. Results and discussion

3.1. $^7Li(p,n)^7Be$ neutron yield spectra

The calculated spectra show results similar to Lee since the channel that leads to the beryllium in its excited state and has a threshold of 2.37 MeV represents a minor contribution to the total neutron yield (0.69% in the case of protons of 2.6 MeV). As an example, Fig. 2 shows the differential yield for 2.6 MeV protons on a LiF target. This figure has been obtained from the generated events of MCNP, it thus takes into account not only the yield calculation but also the implementation of MCNP source distribution cards. For this case the total neutron yield is 3.06×10^{11} n/mC.

3.2. Beam shaping assembly optimization

The optimal BSA configuration was found to have the dimensions shown in Table 1. The optimized BSA shows a neutron spectrum (Fig. 3) with energies centered on 10 keV, which is considered the ideal spectrum for deep seated tumors (Bleuel et al., 1998). The neutron flux profiles show that this energy spectrum leads to a maximum in thermal flux at about 4 cm in depth inside the phantom (Fig. 4).

Simulated neutron doses in healthy tissue show that the main components are due to fast neutron collision with the hydrogen in the skin and the boron dose in the brain (Fig. 5).

All the simulations have been done with the boron concentrations of healthy tissue, tumor boron doses have been estimated by multiplying the healthy boron dose by the ratio of concentrations between tumor and healthy brain. Only tumors in brain have been considered since the optimization is for deep tumors and not for skin. After renormalizing the doses in order that the maximum healthy tissue dose is 12.5RBEGy, the total tumor and healthy tissue dose profiles have been obtained (Fig. 6). The normalization factor in this case corresponds to the maximum treatment time of 43 min. The advantage depth (AD), which means the maximum depth at

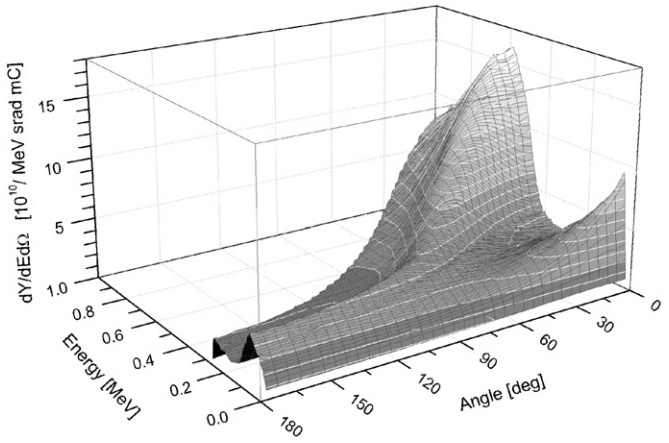

Fig. 2. Example of simulated neutron double differential yield. This case corresponds for 2.6 MeV protons.

Table 1
Parameters for the optimal BSA found in the simulations. For references a, b and c see Fig. 1.

Beam port width (a)	25 cm
Target to the neutron port distance (b)	35 cm
Target to the back of moderator distance (c)	5 cm
Proton beam energy	2.6 MeV

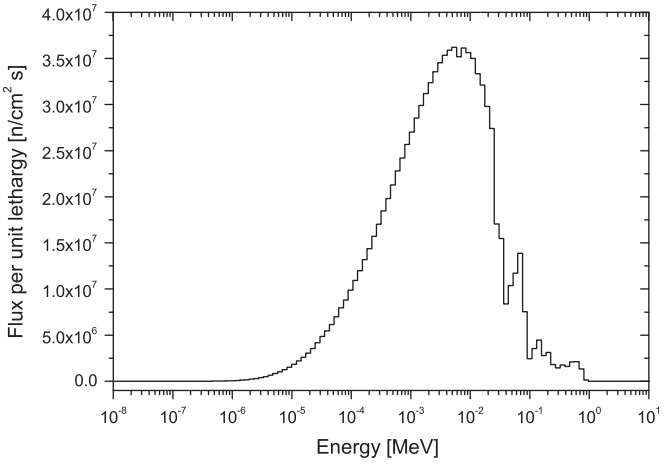

Fig. 3. Energy spectrum simulated at the beam port without phantom.

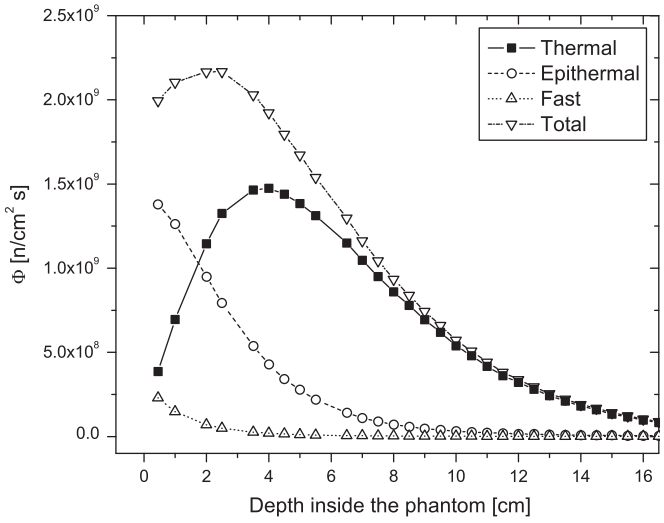

Fig. 4. Neutron flux depth profiles inside the phantom.

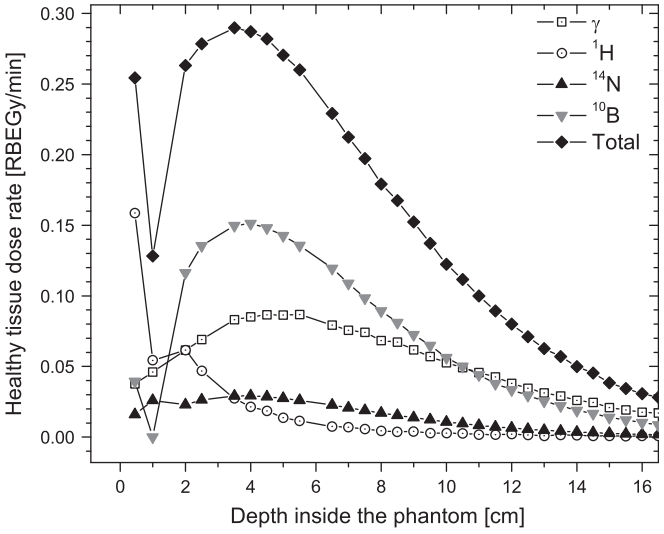

Fig. 5. Depth profiles of the main contributions to the healthy tissue dose rate inside the phantom.

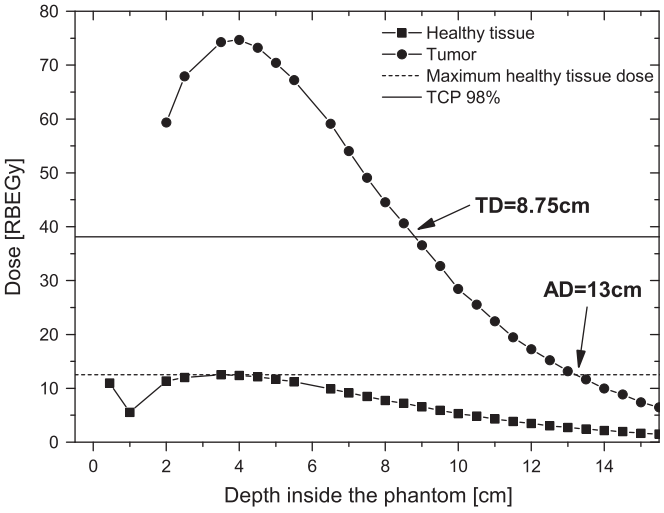

Fig. 6. Total dose-depth profiles inside the phantom for healthy and tumor tissues. A treatable depth (TD) of 8.75 cm and an advantage depth (AD) of 13 cm were obtained.

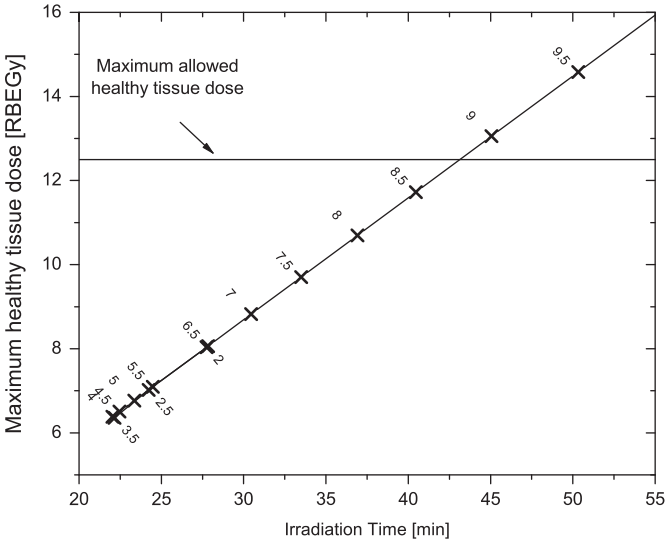

Fig. 7. Figure of merit showing that with this hypothetical BSA and phantom tumors up to 8.75 cm depth can be treated with 98% TCP. Labels indicate the tumor depth in centimeters.

which the tumor dose exceeds the maximum healthy tissue dose is 13 cm. The treatable depth (TD) is the maximum depth for which the tumor dose exceeds 98% in tumor control probability (TCP 98%), in this case $TD = 8.75$ cm.

A possible figure of merit is the one that shows the maximum healthy tissue dose for a TCP of 98% versus the irradiation time for different tumor positions. Fig. 7 shows that tumors up to 8.75 cm can be treated with TCP 98% and irradiation times of less than 45 mins within the tolerance dose of 12.5RBEGy for healthy tissue.

Only the central axis of the phantom has been computed in order to obtain a simple dosimetric study that can be analyzed by automatic scripts. The dose delivered to the skin outside the central axis has not been taken into account and should be studied due to the big neutron beam port. A detailed dosimetric analysis on a clinical glioblastoma case with the optimized configuration found in this work has been performed by Herrera et al. (2010).

4. Conclusions

The results shown in this article for the optimized BSA with the shape and materials considered show good treatment possibilities with short irradiation times (less than 45 min). The beam penetration is excellent: maximum tumor dose at 4 cm depth; 98% TCP up to 8.75 cm depth and an advantage depth of 13 cm.

This work is a starting point for a more exhaustive optimization with different geometry configurations and materials. The dose delivered to skin out of the beam axis has not been evaluated; further work must be made in this sense and in the possible implementation of a beam collimator.

Acknowledgments

A grant from the Agencia Nacional de Promoción Científica y Tecnológica, PAV 22619, is acknowledged.

References

Abramovich, S., et al., 1984. Estimated values of total and differential cross sections of proton interactions with nuclei Li-6 and Li-7. J. Vop. At. Nauki i Tekhn., Ser. Yadernye Konstanty 4, 17.

Binns, P., et al., 2007. Improved dose targeting for clinical epithermal neutron capture beam using optional ^{6}Li filtration. Int. J. Radiat. Onc. Biol. Phys. 67 (5), 1484.

Bleuel D. et al., 1998. Development of a neutron energy-biased in-air figure-of-merit for predicting in-phantom BNCT neutron beam characteristics. In: Proceedings of the Eighth International Symposium on Neutron Capture Therapy for Cancer.

Brown F. et al., 2002. MCNP version 5. Tech. rep. LA-UR-02-3935. Los Alamos National Laboratory Reports.

Goorley, J.T., 2002. Reference dosimetry calculations for neutron capture therapy with comparison of analytical and voxel models. Med. Phys. 29 (2), 145–156.

Herrera et al., 2010. Treatment planning capability assessment of a beam shaping assembly for accelerator based-BNCT, in: Liberman, S. et al. (Eds.), Proceedings of the 14 International Congress on Neutron Capture Therapy, Buenos Aires, pp. 227–230.

ICRU 46, 1992. Photon, electron, proton and neutron interaction data for body tissues. Tech. rep., International Commission on Radiation Units and Measurements.

Kreiner et al., 2010. Development of a tandem-electrostatic-quadrupole facility for accelerator-based boron neutron capture therapy, in: Liberman, S. et al. (Eds.), Proceedings of the 14 International Congress on Neutron Capture Therapy, Buenos Aires, pp. 437–440.

Lee, C.L., Zhou, X.L., 1999. Thick target neutron yields for the ^{7}Li(p,n)^{7}be reaction near threshold. Nucl. Inst. Meth. B. 152 (1), 1–11.

Liskien, H., Paulsen, A., 1975. Neutron production cross sections and energies for the reactions ^{7}Li(p,n)^{7}Be and ^{7}Li(p,n)^{7}Be*. Atomic Data Nucl. Data Tables 15 (1), 57–84.

Sekharan, K.K., et al., 1976. A neutron detector for measurement of total neutron production cross sections. Nucl. Inst. Meth. 133 (2), 253–257.

Ziegler J. et al., 2008. SRIM 2008 PC code.